ARCHIVES OF BIOCHEMISTRY AND BIOPHYSICS
Vol. 294, No. 1, April, pp. 279–281, 1992

Crystallization and Preliminary Analysis of Oxidized, Recombinant, Heterocyst [2Fe–2S] Ferredoxin from *Anabaena* 7120[1]

Bruce L. Jacobson,* Young Kee Chae,‡,§ Herbert Böhme,¶ John L. Markley,§ and Hazel M. Holden*,†,[2]
*Institute for Enzyme Research and †Department of Chemistry, University of Wisconsin, Madison, Wisconsin 53705; ‡Graduate Program in Biophysics and §Department of Biochemistry, University of Wisconsin, Madison, Wisconsin 53706; and ¶Botanisches Institut der Universität Bonn, Bonn, Germany

Received September 26, 1991, and in revised form December 11, 1991

The [2Fe–2S] ferredoxin produced in the heterocyst cells of *Anabaena* 7120 plays a key role in nitrogen fixation, where it serves as an electron acceptor from various sources and an electron donor to nitrogenase. Crystals of recombinant heterocyst ferredoxin, coded for by the *fdx H* gene from *Anabaena* 7120 and overproduced in *Escherichia coli*, have been grown from ammonium sulfate solutions and are suitable for high resolution X-ray crystallographic analysis. They belong to the hexagonal space group $P6_1$ or $P6_5$ with unit cell dimensions of $a = b = 44.2$ Å and $c = 80.6$ Å. The crystals contain one molecule per asymmetric unit and diffract to a nominal resolution of 1.6 Å. The molecular structure of this heterocyst ferredoxin is of special interest in that 4 of the 22 amino acid positions thought to be absolutely conserved in nonhalophilic ferredoxins are different and, based on amino acid sequence alignments, three of these positions are located in the metal-cluster binding loop. Consequently, a high-resolution X-ray analysis of this [2Fe–2S] ferredoxin, and subsequent three-dimensional comparisons with other known ferredoxin models, will provide new insight into structure/function relationships for this class of redox proteins. © 1992 Academic Press, Inc.

The [2Fe–2S] ferredoxins are typically low molecular weight proteins displaying oxidation-reduction potentials between -305 and -455 mV (1). They are involved in a variety of metabolic pathways, including photosynthetic electron transport (2) and nitrogen fixation (3). The first three-dimensional structure of a [2Fe–2S] ferredoxin to be determined by X-ray crystallography was that isolated from the blue–green alga *Spirulina platensis* (4, 5). The model for the protein was never refined, however, and there were difficulties with the structure, particularly in the coordination geometry of the cluster irons and in an extended loop region delineated by amino acid residues 57 to 61. The three-dimensional structures of two other cyanobacterium ferredoxins have now been solved by X-ray analysis: the molecule from *Aphanothece sacrum* (6) and the protein from the vegetative form of *Anabaena* 7120 (7). The main secondary structural elements found in these proteins include two α-helices, a helical turn, and four strands of β-pleated sheet. In both proteins, the metal cluster is located toward the outer edge of the molecule with its iron atoms tetrahedrally coordinated by both inorganic sulfurs and sulfurs provided by protein cysteine residues.

Two biochemically distinct [2Fe–2S] ferredoxins have been purified and characterized from *Anabaena* 7120 (8, 9) and, recently, the structural genes for these ferredoxins (*pet F* and *fdx H*) have been isolated and sequenced (10, 11). The ferredoxin encoded by *pet F* is expressed in vegetative cells and in low levels in heterocysts and couples photosynthetic electron transport to a variety of redox reactions. In contrast, the product of *fdx H* is restricted to heterocysts, specialized cells involved in aerobic nitrogen fixation (10). The heterocyst ferredoxin acts as an immediate electron donor to nitrogenase. The vegetative and heterocyst ferredoxins also differ in midpoint oxidation-reduction potentials, amino acid compositions, immunological cross-reactivities, and electron spin resonance spectra (9). A comparison of their amino acid sequences reveals only 51 of 98 residues to be conserved, thus corresponding to a 52% homology in primary struc-

[1] This research was supported in part by grants from the NIH (GM39082 to H.M.H. and GM35976 to J.L.M.) and Grant 1104 from the New Energy and Industrial Development Organization of Japan (to J.L.M.). H.M.H. is an Established Investigator of the American Heart Association.

[2] To whom correspondence should be addressed.

0003-9861/92 $3.00
Copyright © 1992 by Academic Press, Inc.
All rights of reproduction in any form reserved.

ture. In addition, the heterocyst protein differs from other plant-type [2Fe–2S] ferredoxins in 4 of the 22 positions that are absolutely conserved in the nonhalophilic ferredoxin sequences compared by Matsubara and Hase (12).

As described above, the X-ray structure for the vegetative ferredoxin from *Anabaena* is known and is presently being refined to a resolution of 1.7 Å in our laboratory. In this report, we describe the crystallization and preliminary analysis of the heterocyst molecule. A high resolution X-ray analysis of this protein, and the subsequent comparison of its structure to that of the vegetative form, will provide unique insight into the factors that modulate oxidation-reduction potentials, electron spin resonances, and protein folding for this class of iron–sulfur proteins. In addition, a comparison of the surface topologies of these ferredoxins will help to identify those general areas involved in their interactions with respective physiological redox partners.

MATERIALS AND METHODS

Preparation of recombinant Anabaena 7120 heterocyst ferredoxin. The cloned structural gene for heterocyst ferredoxin (*fdx H*) (10) in a pUC plasmid (13) was subcloned into plasmid pGEM3Zf(−) behind the T7 promoter by cutting both plasmids with *Eco*RI and religating. The resulting plasmid, in which the heterocyst ferredoxin gene is under control of the T7 promoter, was named *pYC*. A second plasmid *pGp1*-2 (Kan^R) contained the T7 polymerase gene under control of the heat-sensitive λ_{PL} promoter (14). *E. coli* strain TG1 transformed with both plasmids was grown overnight in YT medium containing 150 μg/liter ampicillin and 50 μg/liter kanamycin. A 10-ml inoculum of this culture was added to 1 liter of the same medium, and cells were grown at 30°C with shaking until the OD_{600} reached 1.0–1.2. Production of ferredoxin was initiated by shifting the temperature from 30 to 42°C. After 3 h of growth at 42°C, the cells were harvested by centrifugation and then washed by suspending the pellet in 25 mM Tris buffer (pH 8.5) and centrifuging again. The cells were resuspended in the same buffer and disrupted with a French press. Solid urea (Mallinckrodt) was added to the lysate to a final concentration of 8 M to fully denature all holoferredoxin present. DTT[3] was added to a final concentration of about 100 mM to reduce the disulfides and then excess amounts of $FeCl_2$ and Na_2S were added for reconstitution of the iron–sulfur cluster. After about 10 min of flushing with argon, the reaction mixture was diluted eightfold with degassed 25 mM Tris buffer (pH 8.5). Undegassed Tris buffer (same concentration and pH) was added to oxidize the nascent cluster. Subsequently, the mixture was loaded quickly onto a DE53 (Whatman) anion-exchange column (3 cm diameter × 5 cm length) which was washed with 0.1 M NaCl in 25 mM Tris buffer (pH 8.5) and eluted with 1 M NaCl in the same buffer. The crude extract was purified on a Q-Sepharose (Pharmacia) column (3 cm diameter × 10 cm length). Gradient elution with 0.2–0.6 M NaCl (in 10 mM phosphate buffer, pH 7.5) was repeated three times. Each time fractions with higher A_{422}/A_{276} were collected: 0.5, 0.65, and 0.72 on the third run, which represents >95% purity. The final fraction was dialyzed and lyophilized. The yield of purified ferredoxin was approximately 20 mg/liter culture. A 20-mg sample of the heterocyst ferredoxin was used for crystallization trials.

Crystallization experiments. A survey of potential crystallization conditions was conducted at both room temperature and 4°C with the hanging drop method of vapor diffusion (15). All experiments were done in the presence of atmospheric oxygen. The protein concentration was typically 20 mg/ml in 50 mM bis-tris-propane at pH 7.0. Both ammonium sulfate and polyethylene glycol 8000 solutions ranging in pH from 4.5 to 9.0 were tested as possible precipitants.

For X-ray diffraction experiments, crystals were mounted in thin-walled quartz capillary tubes. Diffraction patterns were recorded at 4°C with nickel-filtered copper $K\alpha$ radiation from a Rigaku RU 200 rotating anode X-ray generator operated at 50 kV and 50 mA with a 200-μm focal cup. The exposure time was typically 20 h for a 13° precession photograph at a crystal-to-film distance of 100 mm.

RESULTS AND DISCUSSION

Crystals of the heterocyst ferredoxin were first observed in either ammonium sulfate or polyethylene glycol 8000 solutions buffered with 50 mM succinate, pH 4.5. While the crystals from 16 to 18% polyethylene glycol grew as small thin plates, those from ammonium sulfate often achieved maximum dimensions of 0.6 × 0.6 × 0.6 mm in 3 days. Consequently, crystals are now routinely grown from 2.2 M ammonium sulfate and 50 mM sodium succinate, pH 4.5, at room temperature. Interestingly, while the [2Fe–2S] ferredoxins are acid labile, only those crystallization experiments conducted at pH 5.0 or below yielded crystals.

The heterocyst crystals belong to the space group $P6_1$ or $P6_5$ with unit cell dimensions of $a = b = 44.2$ Å and $c = 80.6$ Å. Assuming one molecule per asymmetric unit and a molecular weight of approximately 11,000, the solvent parameter V_m is 2.06 $Å^3$/Da and is in good agreement with the most commonly observed value of 2.15 $Å^3$/Da (16). Based on still setting photographs, the crystals diffract to at least 1.6 Å resolution. They are physically robust and are stable in the X-ray beam for more than 60 h. Typical 13° precession photographs recorded from these crystals are shown in Figs. 1a and 1b. The limit of diffraction on these photographs is 3.4 Å and as can be seen there is little falloff in intensity at this resolution. A three-dimensional native X-ray data set has been collected with a Siemens area detector system and contains 92% of the total theoretical number of observations to 1.6 Å resolution. The R_{sym} for these data is 4.2%, where $R_{sym} = \Sigma|I - \bar{I}|/\Sigma I$ and measures the agreement between symmetry-related reflections. Within the resolution range of 1.7 to 1.6 Å, 20% of the X-ray intensities are greater than 3σ.

The vegetative and heterocyst ferredoxins from *Anabaena* represent ideal laboratory model systems for understanding the subtle nuances that define structure/function relationships. Once the high resolution three-dimensional structure of the heterocyst molecule is known, it will be possible to compare in detail these two different proteins and to answer many of the structural questions. For example, in the vegetative ferredoxin, there exists an array of ordered water molecules surrounding an exposed phenylalanine side chain (17). Is this solvent pattern around an exposed aromatic residue also observed in the heterocyst protein? The midpoint oxidation-reduction potentials for these two proteins differ by approximately 30 mV. Is the

[3] Abbreviations used: DTT, dithiothreitol; bis-tris-propane; {1,3-bis[tris(hydroxymethyl)methylamino]propane}.

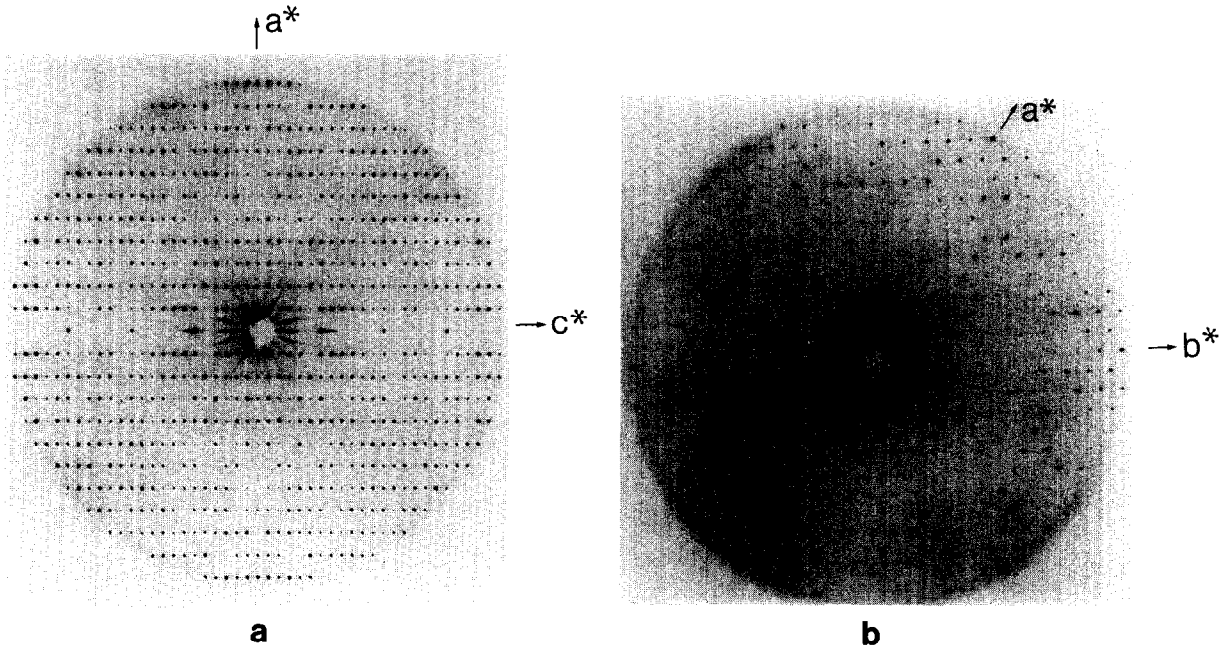

FIG. 1. 13° precession photographs of the *h0l* and *hk*0 zones. The X-ray photographs were recorded from a crystal of dimensions 0.5 × 0.5 × 0.5 mm with nickel-filtered copper $K\alpha$ radiation from a Rigaku RU 200 rotating anode X-ray generator operated at 40 kV and 50 mA with a 200-μm focal cup. The crystal-to-film distance was 100 mm and the collimator size was 0.5 mm. (a) The *h0l* zone shown here was recorded with an exposure time of 17 h. (b) The *hk*0 zone was recorded with an exposure time of 22 h.

hydrogen bonding pattern of the backbone amide hydrogens to the sulfurs in the cluster the same in both forms of the protein? Is there any correlation between the number of aromatic, hydrophobic, and hydrophilic side chains surrounding the cluster and the observed redox potentials for each protein? Do the metal centers in each protein experience the same extent of solvent exposure? The role of Arg 42 in stabilizing the [2Fe–2S] cluster binding loop is clearly defined in the *Anabaena* vegetative structure, where it forms a salt bridge to Glu 31 (17). This arginine is strictly conserved in 22 of 24 nonhalophilic plant-type [2Fe–2S] ferredoxins reviewed by Matsubara and Hase (12). Moreover, Tsukihara *et al.* (5) recognized the potential importance of this residue in folding and function. Yet, in the heterocyst protein, this residue is a histidine. What types of local rearrangements must occur in the heterocyst molecule to accommodate a histidine residue and do these structural changes play a role in the modulation of the electron transport rates and oxidation-reduction potentials? These and many more questions will be addressed once the high resolution structure of the heterocyst ferredoxin from *Anabaena* 7120 is known.

REFERENCES

1. Cammack, R., Rao, K. K., Bargeron, C. P., Hutson, K. G., Andrew, P. W., and Rogers, L. J. (1977) *Biochem. J.* **168,** 205–209.
2. Trebst, A., and Avron, M. (Eds.) (1977) Photosynthesis. I. Photosynthetic Electron Transport and Photophosphorylation, Springer-Verlag, New York.
3. Böhme, H., and Schrautemeier, B. (1987) *Biochim. Biophys. Acta* **891,** 115–120.
4. Fukuyama, K., Hase, T., Matsumoto, S., Tsukihara, T., Katsube, Y., Tanaka, N., Kakudo, M., Wada, I., and Matsubara, H. (1980) *Nature* **286,** 522–523.
5. Tsukihara, T., Fukuyama, K., Nakamura, M., Katsube, Y., Tanaka, N., Kakudo, M., Wada, K., Hase, T., and Matusbara, H. (1981) *J. Biochem.* **90,** 1763–1773.
6. Tsukihara, T., Fukuyama, K., Mizushima, M., Harioka, T., Kusunoki, M., Katsube, Y., Hase, T., and Matsubara, H. (1990) *J. Mol. Biol.* **216,** 399–410.
7. Rypniewski, W. R., Breiter, D. R., Benning, M. M., Wesenberg, G., Oh, B.-H., Markley, J. L., Rayment, I., and Holden, H. M. (1991) *Biochemistry* **30,** 4126–4131.
8. Schrautemeier, B., and Böhme, H. (1985) *FEBS Lett.* **184,** 304–308.
9. Böhme, H., and Schrautemeier, B. (1987) *Biochim. Biophys. Acta* **891,** 1–7.
10. Böhme, H., and Haselkorn, R. (1989) *Mol. Gen. Genet.* **214,** 278–285.
11. Alam, J., Whitaker, R. R., Krogmann, D. W., and Curtis, S. E. (1986) *J. Bacteriol.* **168,** 1265–1271.
12. Matsubara, H., and Hase, T. (1983) Proteins and Nucleic Acids in Plant Systematics (Jensen, U., and Fairbrothers, D. E., Eds.), pp. 168–181, Springer-Verlag, Berlin.
13. Böhme, H., and Haselkorn, R. (1989) *Plant Mol. Biol.* **12,** 667–672.
14. Tabor, S., and Richardson, C. C. (1985) *Proc. Natl. Acad. Sci. USA* **82,** 1074–1078.
15. McPherson, A. (1982) Preparation and Analysis of Protein Crystals, Wiley-Interscience, New York.
16. Matthews, B. W. (1968) *J. Mol. Biol.* **33,** 491–497.
17. Jacobson, B. L., and Holden, H. M. (1991) manuscript in preparation